

Level density within a micro-macroscopic approach

A.G. Magner^{a,*}, A.I. Sanzhur^a, S.N. Fedotkin^a, A.I. Levon^a, S. Shlomo^b

^a*Institute for Nuclear Research, 03680 Kyiv, Ukraine*

^b*Cyclotron Institute, Texas A&M University, College Station, Texas 77843, USA*

Abstract

Statistical level density $\rho(E, A)$ is derived for nucleonic system with a given energy E , particle number A and other integrals of motion in the mean-field approximation beyond the standard saddle-point method (SPM). This level density reaches the two limits; the well-known SPM grand-canonical ensemble limit for a large entropy S related to large excitation energies, and the finite micro-canonical limit for a small combinatorial entropy S at low excitation energies. The inverse level density parameter K as function of the particle number A in the semiclassical periodic orbit theory, taking into account shell effects, is calculated and compared with experimental data.

Keywords: level density, shell effects, Thomas-Fermi approach, periodic orbit theory, neutron resonances.

1. Introduction

Many properties of heavy nuclei can be to large extent described in terms of the statistical level density [1–16]. Usually, the level density $\rho(E, A)$, where E and A , are the energy and nucleon number, respectively, is calculated by the inverse Laplace transformation of the partition function $\mathcal{Z}(\beta, \alpha)$ of the corresponding Lagrange multipliers. Other integrals of motion, e.g., the orbital angular momentum projection M , or separately, the number of neutrons and protons instead of A can be considered in a similar way by introducing other Lagrange multipliers. Within the grand canonical ensemble, the standard saddle-point method (SPM) was used for the integration over all variables, including β , which is related to the total energy E [2, 4]. This method assumes a large excitation energy U , so that the temperature T can be defined through a well-determined saddle point in the integration variable β for a finite Fermi system of large particle numbers. However, many experimental data are related also to the low-lying part of the excitation energy U , where such a saddle point does not exist. For presentation of experimental data on nuclear spectra, the cumulative number of quantum levels below a given excitation energy U is conveniently often used for a statistical analysis [17–19], e.g., of the experimental data on the collective excitation energies of rare-earth and actinide nuclei excited in two-neutron transfer (p,t) reactions [20]. For calculations of this cumulative number one has to integrate the level density over a large interval of the excitation energy U from small values where there is no thermodynamical equilibrium to large values where the standard approach can be successfully applied in terms of the temperature T in a finite Fermi system. Therefore, to simplify the level density, $\rho(E, A)$, calculations we will integrate over the Lagrange multiplier β in the inverse Laplace transformation of the partition function $\mathcal{Z}(\beta, \alpha)$ more exactly beyond the SPM. It is worthwhile to unify the standard Fermi-gas model for large excitation energies U with the empiric constant temperature model (CTM) at small U as suggested in Ref. [3], see also Ref. [21].

Such a micro-macroscopic approximation (MMA) which unifies micro- and macroscopic ensembles, for the statistical level density ρ was suggested in Ref. [22]. A simple expression of ρ in terms of the modified Bessel function of the entropy variable was obtained for a small heat excitation energy U as compared to the rotational excitations E_{rot} within the mean field approach. The shell-correction method (SCM) [23], was applied [22] for studying the shell effects in the nuclear moment of inertia. For a deeper understanding of the correspondence between the classical and

*Corresponding author

Email address: magner@kinr.kiev.ua (A.G. Magner)

the quantum approach, it is also worthwhile to analyze the shell effects in the level density ρ within the semiclassical periodic-orbit theory (POT) [24–28].

In the present study we extend the MMA approach [22] for the description of shell effects in terms of the level density itself for larger excitation energies U . The level density parameter a is one of the key quantities under intensive experimental and theoretical discussions [6, 8, 11, 13, 14, 16]. Smooth properties of the inverse level density, $K = A/a$, as function of the nucleon number A have been studied within the framework of the self-consistent Extended Thomas-Fermi ((E)TF) approach [8, 14]. However, shell effects in the statistical level density is still an attractive subject, especially important near nuclear magic numbers.

2. Micro-macroscopic approach

For a statistical description of level density of a nucleus in terms of the conservation variables – the total energy, E , and nucleon number, A , one can begin with the micro-canonical expression for the level density,

$$\rho(E, A) = \sum_i \delta(E - E_i) \delta(A - A_i) \equiv \int \frac{d\beta d\alpha}{(2\pi i)^2} e^S, \quad (1)$$

where E_i and A_i present the system spectrum, $S = \ln \mathcal{Z}(\beta, \alpha) + \beta E - \alpha A$ is the entropy with $\mathcal{Z}(\beta, \alpha)$ being the partition function. Integrating over α for a given β by the standard SPM in Eq. (1), we use the expansion for this entropy as: $S(\beta, \alpha) = S(\beta, \alpha^*) + (\partial^2 S / \partial \alpha^2)^* (\alpha - \alpha^*)^2 / 2 + \dots$. The first order term of this expansion disappears because the Lagrange multiplier, α^* , is defined by the saddle point (SP) condition,

$$\left(\frac{\partial S}{\partial \alpha} \right)^* \equiv \left(\frac{\partial \ln \mathcal{Z}}{\partial \alpha} \right)^* - A = 0. \quad (2)$$

Thus, this equation determines the chemical potential, $\lambda = \alpha^* / \beta$, as function of the particle number A .

Introducing, for convenience, the potential $\Omega = -\ln \mathcal{Z} / \beta$, one can define the system partition function \mathcal{Z} through

$$\Omega = \mathcal{E} - \frac{a}{\beta^2}, \quad \mathcal{E} = E_0 - \lambda A, \quad (3)$$

where E_0 is the energy of a non-excited system, ground state or that including a collective (e.g., rotational) motion, a is the level density parameter. Substituting the expansion of the entropy near the SP into Eq. (1), and taking the error integral over α in the extended infinite limits, one obtains

$$\rho(E, A) \approx \int \frac{d\beta \beta^{1/2}}{2\pi i \sqrt{2\pi}} \mathcal{J}^{-1/2} \exp\left(\beta U + \frac{a}{\beta}\right), \quad (4)$$

where $U = E - E_0$ is the excitation energy. In the thermodynamic limit for a large excitation energy U one finds the temperature $T = 1/\beta^*$ through the saddle point $\beta = \beta^*$, and the well-known expression for the grand-canonical potential Ω . In Eq. (4), the one-dimensional Jacobian determinant \mathcal{J} (c number) is taken at the saddle point (2),

$$\mathcal{J} \equiv \beta \left(\frac{\partial^2 S}{\partial \alpha^2} \right)^* \equiv - \left(\frac{\partial^2 \Omega}{\partial \lambda^2} \right)^* = \mathcal{J}_\infty + \mathcal{D}_\beta, \quad \mathcal{J}_\infty = - \frac{\partial^2 \mathcal{E}}{\partial \lambda^2}, \quad \mathcal{D}_\beta = \frac{1}{\beta^2} \frac{\partial^2 a}{\partial \lambda^2}. \quad (5)$$

The level density parameter a can be expressed in terms of the single-particle (s.p.) level density $g(\lambda)$,

$$a = \frac{\pi^2}{6} g(\lambda), \quad g(\lambda) = \tilde{g}(\lambda) + \delta g(\lambda), \quad (6)$$

where $\tilde{g}(\varepsilon)$ is Strutinsky smooth s.p. level density, approximately equal to the (E)TF one (including the spin or spin-isospin degeneracy), and $\delta g(\varepsilon)$ is the oscillating (shell) component which can be calculated using the SCM [23] or semiclassically within the periodic orbit theory [25, 27], both taken at the chemical potential $\varepsilon = \lambda$. Using the Fermi-gas grand-canonical expressions for the energy E_0 and particle number A in terms of the s.p. level density, $g(\varepsilon)$,

$E_0 = \int_0^\lambda d\varepsilon \varepsilon g(\varepsilon)$ (Refs. [23, 27]) and $A = \int_0^\lambda d\varepsilon g(\varepsilon)$, for the Jacobian component \mathcal{J}_∞ one has [4] $\mathcal{J} \cong \mathcal{J}_\infty \approx g(\lambda)$. According to Eq. (6), for the second term (5) of the Jacobian \mathcal{J} one writes $\mathcal{D}_\beta = (\pi^2/6)g''(\lambda)/\beta^2$. The critical quantity for following derivations is their ratio:

$$\xi = \mathcal{D}_\beta/\mathcal{J}_\infty \approx -(\pi^2/6)\delta g''(\lambda)/\beta^2 \tilde{g} \sim (T/\lambda)^2 (2\pi A^{1/3})^4 \delta E/E_{\text{ETF}}, \quad (7)$$

where $T = 1/\beta^*$ is the temperature evaluated at the saddle point $\beta = \beta^*$, δE is the semiclassical POT energy shell correction, $\delta E \approx (D_{\text{sh}}/(2\pi))^2 \delta g(\lambda)$, for major shell structure [25–28], E_{ETF} is the smooth ETF energy, $E_{\text{ETF}} \sim \tilde{g}(\lambda)\lambda^2$, $D_{\text{sh}} \approx \lambda/A^{1/3}$ is the mean distance between major shells ($\delta g'' \approx -(2\pi/D_{\text{sh}})^2 \delta g$). For typical parameters $\lambda = 40$ MeV, $A \sim 200$, and $\delta E/E_{\text{ETF}} \sim 10^{-2}$ [23], one finds the estimate $\xi \sim 0.1 - 10$ for temperatures $T \sim 0.1 - 1$ MeV. In line of the SCM [23] and ETF approach [27], these values are given finally using the realistic smooth energy E_{ETF} for which the binding energy approximately equals $E_{\text{ETF}} + \delta E$.

For calculations of the Jacobian \mathcal{J} , Eq. (5), we will consider two different limiting cases. In the case (i) of small contribution of the β -dependent component \mathcal{D}_β of the Jacobian (5), $\xi \ll 1$, Eq. (7), that is related to small heat excitations with respect to the collective (rotational) motion, we will approximate the Jacobian \mathcal{J} by the constant \mathcal{J}_∞ (independent of β), $\mathcal{J} \approx \mathcal{J}_\infty$. Then, one takes the Jacobian factor $\mathcal{J}^{-1/2}$ off the integral in Eq. (4), done as in Ref. [22]. Transforming β to a new variable $\tau = 1/\beta$, we recognize in Eq. (4) the standard Laplace transform. Calculating this integral over τ , one finally arrives at

$$\rho \approx \rho_{\text{MMA}}(S) = \bar{\rho}_\nu f_\nu(S), \quad f_\nu(S) = S^{-\nu} I_\nu(S), \quad (8)$$

where S is the Fermi-gas (mean-field) entropy, $S = 2\sqrt{aU}$, with U being the excitation energy defined above, $U = E - E_0$. In Eq. (8), $\bar{\rho}_\nu$ is a constant, independent of the entropy S , $\bar{\rho}_\nu = 2a^\nu \pi^{1-\nu} |\mathcal{J}_\infty^{(2\nu-2)}|^{-1/2}$, where $2\nu - 2$ is the determinant dimension (superscript one is omitted in Eq. (5)). The modified Bessel function $I_\nu(S)$ of the order of ν , $\nu = (n+1)/2$, is determined by the number of integrals of motion n ($n = 2$, and therefore, $\nu = 3/2$ for this case of the two integrals of motion E and A). Expression (8) is written in a general form for arbitrary number of integrals of motion n . For the specific case $n = 2$ here ($\nu = 3/2$), one obtains

$$\rho(E, A) = a\sqrt{2\pi/3} I_{3/2}(S)/S^{3/2}, \quad (9)$$

see Ref. [22] for the case of $n = 3$ ($\nu = 2$, $\rho = \rho(E, A, M)$) in Eq. (8). The asymptotics for large entropy S is given by

$$f_\nu(S) = \frac{\exp(S)}{S^\nu \sqrt{2\pi S}} \left[1 + \frac{1-4\nu^2}{8S} + \mathcal{O}\left(\frac{1}{S^2}\right) \right]. \quad (10)$$

This approximation at zero order in expansion over $1/S$ is identical to that obtained directly from Eq. (4) by the SPM over all variables. At small entropy, $S \ll 1$, one obtains also from Eq. (8) the finite combinatoric power expansion:

$$f_\nu(S) = \frac{2^{-\nu}}{\Gamma(\nu+1)} \left[1 + \frac{S^2}{4(\nu+1)} + \mathcal{O}(S^4) \right], \quad (11)$$

where $\Gamma(x)$ is the Gamma function. This expansion over powers of $S^2 \propto U$ is the same as that of the ‘‘constant temperature model’’ (CTM) [3, 21], used often for the level density calculations at small excitation energies U , but here we have it without free parameters. Using the asymptotics of Eq. (10) in Eq. (9) for large S , one arrives at the Bethe expression for the level density [1, 2, 4]. This asymptotic expression is obviously divergent at $U \rightarrow 0$, in contrast to the finite MMA limit (11) for the level density, Eq. (8).

In the opposite case (ii), $\xi \gg 1$, see Eq. (7) for a relatively large heat excitation energy, one obtains for the Jacobian, Eq. (5), $\mathcal{J} \approx \mathcal{D}_\beta \approx (\pi/6)^2 g''(\lambda)/\beta^2$. The inverse Laplace integrand requires the additional power of β . Therefore, after transformation of the variable, $\beta = 1/\tau$, and taking explicitly the inverse Laplace transform we arrive at Eq. (8) with $\nu = 5/2$,

$$\rho(E, A) = \bar{\rho}_{5/2} S^{-5/2} I_{5/2}(S), \quad \bar{\rho}_{5/2} = \frac{4\sqrt{2}\lambda^{3/2}a^{5/2}}{\pi^{3/2}A^{1/2}}. \quad (12)$$

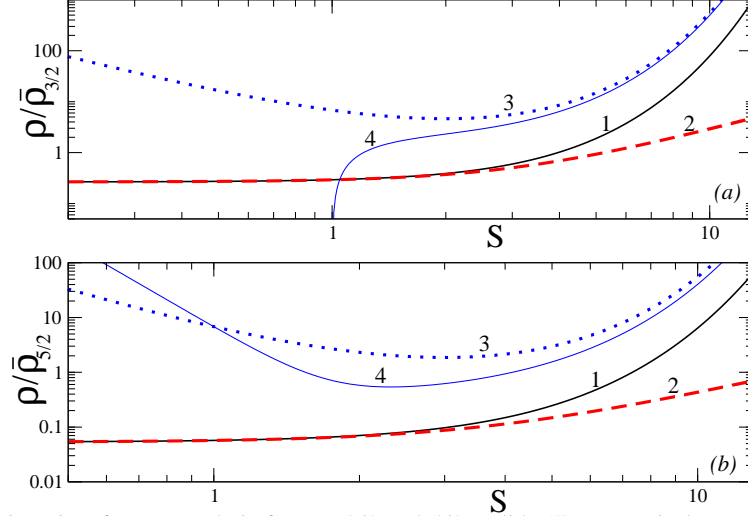


Figure 1: Level density ρ in units of $\bar{\rho}_\nu$, (a) and (b) for $\nu = 3/2$ and $5/2$ (solid “1”), respectively, are shown as functions of the entropy S in different approximations: 1) $S \ll 1$ (dashed “2”, Eq. (11), and 2) $S \gg 1$ (dots and thin solid), Eq. (10), “3” and “4”, are expansions over $1/S$ up to zero and first [in (a)] or second [in (b)] order terms in Eq. (10), respectively.

In this case for the level density $\rho(E, A, M)$, one obtains the same Eq. (8) but with $\nu = 3$ and $\bar{\rho}_3 \approx (4\sqrt{2}a^3\hbar/\pi^2)(\lambda^3/A\Theta)^{1/2}$ in Eq. (8), where Θ is the moment of inertia, which is approximated by the TF nuclear moment of inertia Θ_{TF} , $\Theta \approx \Theta_{\text{TF}}$. The values of ν in the case (ii) correspond to $\nu - 1$ of the case (i).

In Fig. 1 we show the level density dependence $\rho(S)$ [Eq. (8), for $\nu = 3/2$ in (a) and $\nu = 5/2$ in (b) panels] on the entropy variable S and its different asymptotics. In this figure, a small [$S \ll 1$, Eq. (11)] and large [$S \gg 1$, Eq. (10)] entropy S behavior is presented. For large $S \gg 1$ we neglected the corrections of the inverse power expansion of the pre-exponent factor in square brackets of Eq. (10), lines “3”, and took into account the corrections of the first [$\nu = 3/2$, (a)] and up to second [$\nu = 5/2$, (b)] order in $1/S$ to show their slow convergence to the exact MMA result “1” (8). It is interesting to find almost a parallel constant shift of the simplest, $\rho \propto \exp(S)/S^\nu$, SPM asymptotic approximation at large S (dots “3”) with respect to the solid curve of the exact MMA result (8). This may clarify one of the phenomenological models, e.g., the back-shifted Fermi-gas (BSFG) model for the level density [7, 11, 29].

From Eq. (8) one can calculate the level density $\rho(E, A, I)$ with a given energy E and the total angular momentum I in terms of the Bessel functions, $\rho(E, A, I) = -\partial\rho(E, A, M)/\partial M$ at $M = I + 1/2$ (see Refs. [4, 6, 7]), which is proportional to $I_4(S)/S^4$ in the case (ii). Using also the expansions (11) for $S \ll 1$ and (10) for $S \gg 1$ over S of the Bessel functions, one finds a finite combinatoric (CTM) and SPM limit expressions. The main term of these expressions for $S \gg 1$ coincides with the SPM limit. For small angular momentum I and large excitation energy $U_0 \approx E - E_0$, $I(I+1)\hbar^2/2\Theta U_0 \ll 1$, $\Theta \approx \Theta_{\text{TF}}$, one finds, e.g., in the case (ii) the separation of the level density into the product of spin-dependent, $f(I)$, and excitation-energy, U_0 , factors,

$$\rho(E, A, I) = \frac{\bar{\rho}_3 f(I) \exp(2\sqrt{aU_0})}{32\sqrt{\pi}a^{5/4}U_0^{9/2}}, \quad f(I) = \frac{\hbar^2(2I+1)}{\Theta} \exp\left(-\frac{I(I+1)\hbar^2\sqrt{a}}{2\Theta\sqrt{U_0}}\right). \quad (13)$$

The power dependence of the pre-exponent level density $\rho(E, A, I)$ on the excitation energy $E - E_0$ differs from that of $\rho(E, A, M)$, while one has the same exponential dependence $\rho \propto \exp(2\sqrt{a(E - E_0)})$ for a large excitation energy $E - E_0$ and small angular momentum I . Integrating Eq. (13) over I (with accounting for the spin degeneracy), one has the expression for $\rho(E, A)$ (ii) which is assumed to be valid for large excitation energies U and small nuclear spins (Fermi-gas small spin (FGSS) model),

$$\rho(E, A) = \frac{a\lambda^{3/2}}{2\pi^2\sqrt{A}U_0^{3/2}} \exp(2\sqrt{aU_0}). \quad (14)$$

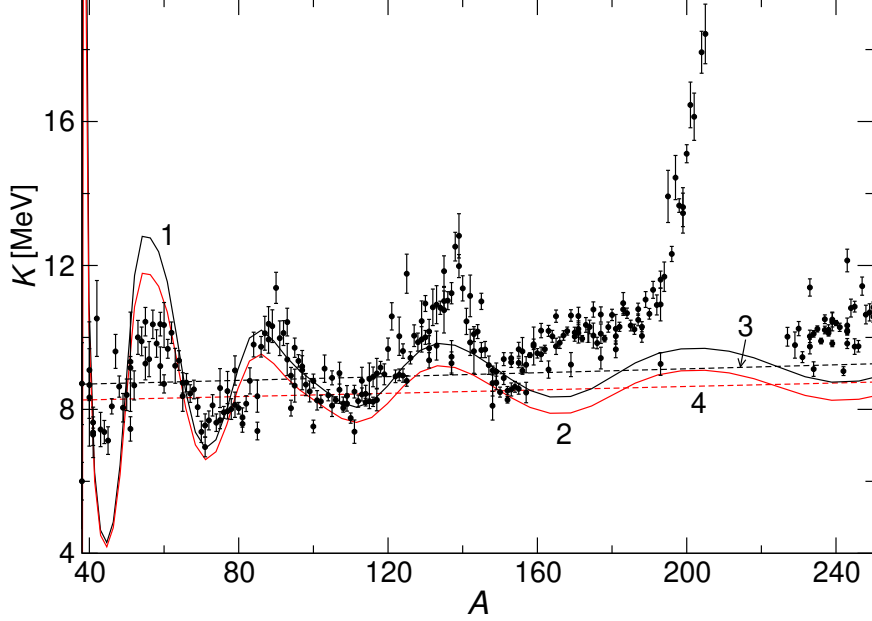


Figure 2: The inverse level-density parameter $K = A/a$ (solids “1” for SKM* and “2” for KDE0v1 forces) is shown as function of the particle number A . The smooth part in the ETF approach is taken from Ref. [14] for these two versions of the Skyrme forces SKM* (“3” dashed) and KDE0v1 (“4” dashed). The solid oscillating curves are obtained by using the semiclassical POT approximation, Eq. (15), for the level density shell corrections at Gauss width averaging parameter $\gamma = 0.3$, and dashed curves “3” and “4” for a smooth part, both including the effective mass. Experimental values, shown by solid points, are taken from Ref. [11].

3. Results and discussions

Fig. 2 shows the inverse level-density parameter $K = A/a$, with a of Eq. (6) as function of the particle number A in the semiclassical POT approximation. The result of these calculations are largely in a qualitative agreement with the new experimental data [11], which, as compared to Ref. [5], include many other excited nuclei and different reactions with nuclear excitation energies being significantly smaller than the neutron separation energy, were used in the analysis. The sets of levels in the limited energy range below the neutron binding energy with reliable completeness were selected for each nucleus, and neutron resonance densities were included in the analysis. We added the smooth self-consistent ETF values of a for the KDE0v1 [30] and the SkM* [31] Skyrme forces from Refs. [14, 16] to their shell corrections $[\delta g(\lambda)]$ through the total s.p. level density $g(\lambda)$ of Eq. (6). Its oscillating component $\delta g(\lambda)$ was approximated by the analytical POT trace formula [24, 25, 27] for the infinitely deep spherical square-well potential,

$$\delta g_{\text{scl}}(kR) = \frac{2mR^2 d_s}{\hbar^2} \left[\sqrt{\frac{kR}{\pi}} \sum_{p,t} (-1)^t \sin(2\varphi_{pt}) \sqrt{\frac{\sin(\varphi_{pt})}{p}} \sin\left(kL_{pt} - 3p\frac{\pi}{2} + \frac{3\pi}{4}\right) - \sum_t \frac{\sin(4tkR)}{2\pi t} \right], \quad (15)$$

where d_s is spin (spin-isospin) degeneracy, $k = \sqrt{2m\varepsilon/\hbar^2}$ is the wave number, $L_{pt} = 2pR \sin(\varphi_{pt})$ is the PO length, R is the radius of the spherical cavity, $\varphi_{pt} = \pi t/p$, and p and t are the numbers of turning points and rotations around the center of the PO (winding number) in the spherical cavity, respectively. The first and second terms in square brackets of Eq. (15) are the contributions of families of the planar orbits and diameters, respectively. This formula almost identically reproduces the SCM quantum results for the s.p. level density for the same potential [27]. The major shells in Fig. 2 are clearly seen as maxima of $K(A)$, which correspond to minima of the density parameter a , or the oscillating level density component $\delta g(\lambda)$, see Eqs. (6) and (15). The relationship between the chemical potential λ , through $k_F R$, where $\hbar k_F = (2m\lambda)^{1/2} \approx (2m\varepsilon_F)^{1/2}$ is the Fermi momentum, ε_F is the Fermi energy, and m the nucleon mass. The particle numbers A for this potential [25, 27] is given by

$$A = - \left(\frac{\partial \Omega}{\partial \lambda} \right)^* \approx \int_0^\lambda d\varepsilon g(\varepsilon). \quad (16)$$

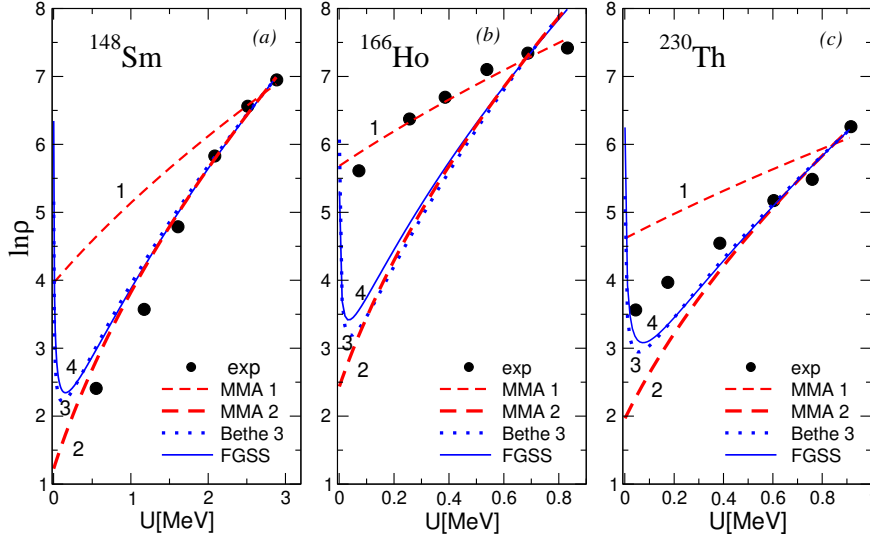


Figure 3: Level density, $\ln\rho(E, A)$, obtained for low energy states in nuclei ^{148}Sm (a), ^{166}Ho (b), and ^{230}Th (c) in different approximations: The MMA “1” and “2” are given by Eqs. (12) and (9) for $\rho(E, A)$, respectively; “3” and “4” are the Bethe [1] and FGSS [3] (Eq. (6)) asymptotics (with the constant chemical potential $\lambda = 40$ MeV, independent of particle numbers), respectively. Experimental dots are obtained from the excited states spectrum of these nuclei (see Ref. [32]) by using the sample method. Similarly, as in the SCM [23], the sample lengths $U_s = 0.45, 0.15,$ and 0.17 MeV are found on the plateaus but over inverse level density parameters K , respectively.

In this transformation, $k_F R$ to A , one can conveniently use the quantum SCM level density [23]. The Gaussian averaging width of the oscillating level density δg in Fig. 2 is the same $\gamma = 0.3$ as that in previous POT calculations [28]. It corresponds to the dimensional Gaussian width $\Gamma \approx 2\gamma\lambda/k_F R \approx 3$ MeV ($\lambda = 40$ MeV, $R = r_0 A^{1/3}$, $r_0 = 1.14$ fm, $A = 100 - 200$). In calculations of Fig. 2, only short planar POs yield main major-shell contributions into the PO sum (15) through the oscillating level density in Eq. (6). Mean value of oscillating $K(A)$ in Fig. 2 is about 8 MeV, $\hbar^2/2mr_0^2 \approx 16$ MeV, as predicted in Ref. [8]. This is in accordance with the ETF (SkM* or KDE0v1) value, accounting for the effective mass m^* . As shown in Ref. [14], the effect of the effective mass m^* on the inverse level density K is strong, decreasing of K by factor about 2, that leads approximately to mean values of the experimental data [11]. However, we should not expect that for the infinitely deep spherical square-well potential the positions of the maxima (minima of a , i.e., of the s.p. level density, $\delta g(\varepsilon)$ at $\varepsilon = \lambda$, related to magic nuclei in that potential) can be correctly reproduced in such shell-correction calculations, first of all, because of neglecting the spin-orbit interaction. As shown in Refs. [26, 28] for semiclassical explanation of the positions of the magic nucleus ^{240}Pu , we should shift the curves $K(A)$ along the A axis [through $k_F R$, Eq. (16)]. Therefore, we shifted the semiclassical curves in Fig. 2 with about $\Delta A = 20$ along the particle number A axis. This shift is of the order of a half of the distance D_{sh} between major shells near the Fermi surface in the particle number variable A (see text below Eq. (7)). According to the POT estimations [25] for the period D_{sh} and TF level density $g_{\text{TF}} = 3A/2\lambda$, one finds for the period of the major shell structure, A_{sh} , in the particle number variable, $A_{\text{sh}} \approx D_{\text{sh}} g_{\text{TF}} \approx 3 A^{2/3}/2$. For $A = 100 - 200$, one obtains $A_{\text{sh}} \approx 30 - 50$, which is of the order of the realistic period of the nuclear major shell structure. The position of a maximum over the particle number variable, as related to the value of $k_F R$, is the only one parameter needed to adjust the semiclassical solid curves with the experimental data. This is similar to the discussions in Ref. [28] where the magic number for ^{240}Pu was obtained semiclassically by using a similar shift. Therefore, three minima of the major shell closures in the semiclassical calculations at $A \approx 45 - 150$ in Fig. 2 correspond to the experimentally obtained maxima. In spite of a very simple explicitly given analytical formula (15) (Refs. [24, 25, 27]) for the s.p. level density shell corrections in the spherical cavity, one obtains largely good agreement of the semiclassical approximation, which is almost identical to the quantum SCM result for the same cavity, to experimental data in this range of nuclear particle numbers A . Magnitudes of periods and amplitudes for the oscillations of $K(A)$ are basically in good agreement.

However, there is a discrepancy between experimental and theoretical results for $K(A)$ in the range of particle numbers $A \approx 150 - 240$. One of possible reasons is that different approximations for the statistical level density ρ are

used in fitting procedure to obtain the experimental prediction of K with respect to those of this MMA approach (8). New information on a , the energy parameter E_1 and the spin-cutoff parameter σ^2 ($\sigma^2 = \Theta \sqrt{U_0/a}/\hbar^2$, where $\Theta \approx \Theta_{\text{TF}}$ in our approximations) were obtained applying the SPM BSFG formula for the level density to the experimental spectra in Ref. [11]. Experimental data for K are in good agreement with those of neutron resonances, see Refs. [5, 14], which are dominating in calculations of Ref. [11]. The specific reason for the discrepancy might be that the density parameter a (or K) was obtained by three parameter (a, E_1 and σ^2) fitting of these experimental data to the level density, $\rho \propto \exp(S)$, in the BSFG approximation. This approximation is not valid for small excitation energies U , in contrast to the MMA approach with the correct zero excitation energy limit. For neutron resonances, one can assume a small angular momentum I and large excitation energy. Apart from a shift of the excitation energy in exponent argument, another source of the discussed discrepancy can be a different pre-exponent dependence of $\rho(E, A, I)$, Eq. (13) (in the (ii) case), on the excitation energy U_0 (at zero angular momentum I) and on the level density parameter a with respect to the level density ρ of the BSFG approach in Ref. [11].

In Fig. 3 we present results of the MMA, Bethe and FGSS approximations to the statistical level density $\rho(E, A)$ (in logarithms) as functions of the excitation energy U versus the experimental data. They are calculated at the inverse level density parameter K deduced from fits to experimental data for several nuclei. The experimental data used for the statistical level density $\rho(E, A)$ are obtained from Ref. [32] for the excitation energies U and spins by using the sample method [7]. In Fig. 3 we present the two opposite situations concerning the states distributions as functions of the excitation energy U . We show results for ^{148}Sm in Fig. 3(a) for the case of almost no states with extremely low excitation energies (LES), as for ^{208}Pb where there is no such levels at all. Only a few levels in ^{148}Sm can be found at $U \lesssim 1$ MeV, which yield entropies $S \lesssim 1$. For ^{166}Ho in Fig. 3(b), one finds the opposite situation when there is a lot of such LESs. An intermediate number of LESs is observed, e.g., in ^{230}Th (Fig. 3(c)). Thus, we present the results for two nuclei, ^{166}Ho and ^{230}Th , from both sides of the desired particle number interval $A \approx 150 - 240$. In Fig. 3, the results of the MMA, Eqs. (12) and (9) (with the approximate TF evaluations of Jacobians \mathcal{J}), are shown by the curves “1” and “2” while “3” and “4” correspond to the Bethe [1] and well-known FGSS asymptotics, respectively [3], Eq. (6). In all panels of Fig. 3, one can see the divergence of the FGSS and the Bethe level densities [1–4] near the zero excitation energy $U \rightarrow 0$, in contrast to the finite combinatoric MMA expressions of Eq. (11) in this limit; see Eqs. (8), (9), and (12). We do not use arbitrary empiric parameters of the BSFG, spin cut-off FGSS and those of the empiric CTM [11]. As an advantage, one has only one parameter K which has a certain physical meaning as the inverse level density parameter. The variations of K are related, e.g., to those of the mean field parameters through Eq. (6). All the densities $\rho(E, A)$ do not depend on the cut-off spin factor and moment of inertia because of summation (integrations) over all spins (with accounting for the degeneracy factor) which could appear in the spectrum. The MMA-1 for ^{166}Ho (see Fig. 3(b)) compared with the results of the MMA-2, Bethe and FGSS approximations, is obviously much better than for ^{148}Sm (Figure 3(a)) for which one has the opposite situation. For ^{230}Th (Figure 3(c)), one obtains the experimental data at LESs in the middle of two limiting cases MMA-1 (i) and MMA-2 (ii).

In line of the results of Ref. [13], the MMA-1 results for K are significantly larger than the MMA-2 ones and those obtained mainly for the neutron resonances (NRs). For MMA-2, one finds K of the same order as that of the Bethe and FGSS approaches. The MMA-2, Bethe and FGSS values of K are mostly close to the NR values in order of magnitude. For the FGSS case it is obviously because NRs occur at large excitation energies U and small spins. Large deformations, neutron-proton asymmetry and pairing correlations [2, 6, 7, 9, 10, 15, 21] of the rare earth and actinide nuclei should be also taken into account to improve the comparison with experimental data.

4. Conclusions

We derived the statistical level density $\rho(S)$ as function of the entropy S within the micro-macroscopic approximation using the mixed micro- and grand-canonical ensembles beyond the standard saddle point method. This function can be applied for small and, relatively, large entropies S or excitation energies U of a nucleus. For a large entropy (excitation energy), one obtains the exponential asymptotics of the standard SPM Fermi-gas model, however, with the significant inverse $1/S$ power corrections. For small S one finds the usual finite combinatoric expansion in powers of S . Functionally, the MMA at linear approximation in S^2 expansion, at small excitation energies, coincides with the empiric constant “temperature” model, but without using free fitting parameters. Thus, MMA unifies the commonly accepted Fermi-gas approximation with the empiric CTM for large and small entropies S , respectively, in line with the suggestions in Refs. [3, 21]. The MMA clearly manifests an advantage over the standard SPM approaches, as

FGSS approach, at low excitation energies, because of no divergences of the MMA in the limit of small excitation energies, in contrast to the FGSS asymptotics. Another advantage takes place for nuclei which have much more states in the very LES range. The values of the inverse level density parameter K are compared with experimental data for LESs below neutron resonances (NRs) in nuclear spectra of several nuclei. The MMA results with only one physical parameter in the least mean-square fitting - inverse level density parameter K - is usually the better the larger number of the extremely low energy states, certainly much better than for the FGSS model in this case. The MMA values of the inverse level density parameter K for LESs can be significantly larger than those of the neutron resonances within the FGSS model. Major shell oscillations of the inverse level density parameter K are compared with modern experimental data, basically for neutron resonances. We found qualitatively good agreement between semiclassical POT and quantum-mechanical results with experimental data on the inverse level density parameter K , after overall shift of all $K(A)$ curves by only one parameter because of the spin-orbit interaction, between particle numbers $A \approx 45 - 150$, where we find many extremely low excitation states.

As perspectives, the neutron-proton asymmetries, large nuclear angular momenta and deformations, as well as pairing correlations, will be taken into account in future work to improve the comparison of the theoretical evaluations with experimental data on the level density parameter significantly below the neutron resonances. Our approach can be applied to the statistical analysis of the experimental data on collective nuclear states.

Acknowledgement

The authors gratefully acknowledge D. Bucurescu, R.K. Bhaduri, M. Brack, A.N. Gorbachenko, and V.A. Plujko for creative discussions. This work was supported in part by the budget program "Support for the development of priority areas of scientific researches", the project of the Academy of Sciences of Ukraine, Code 6541230. S. Shlomo is supported in part by the US Department of Energy under Grant no. DE-FG03-93ER-40773.

References

- [1] H. Bethe, Phys. Rev. **50** (1936) 332.
- [2] T. Ericson, Adv. in Phys. **9** (1960) 425.
- [3] A. Gilbert and A.G.W. Cameron Canadian J. of Phys. **43** (1965) 1446.
- [4] Aa. Bohr and B.R. Mottelson, *Nuclear structure* (Benjamin, New York, 1967) vol I.
- [5] V.S. Stavinsky, Sov. J. Part. Nucl. **3** (1972) 417.
- [6] A.V. Ignatyuk, *Statistical properties of excited atomic nuclei* (Ergoatomizadat, Moscow, 1983 (Russian)).
- [7] Yu.V. Sokolov, *Level density of atomic nuclei* (Ergoatomizadat, Moscow, 1990 (Russian)).
- [8] S. Shlomo, Nucl. Phys. A **539** (1992) 17.
- [9] Y. Alhassid, G.F. Bertsch, S. Liu, and H. Nakada, Phys. Rev. C **84** (2000) 4313.
- [10] Y. Alhassid, G.F. Bertsch, and L. Fang, Phys. Rev. C **68** (2003) 044322.
- [11] T. von Egidy and D. Bucurescu, Phys. Rev. C **78** (2008) 051301(R); **80** (2009) 054310.
- [12] Y. Alhassid, G.F. Bertsch, C.N. Gilbreth, and H. Nakada, Phys. Rev. C **93** (2016) 044320.
- [13] V. Zelevinsky and R. Senkov, Phys. Rev. C **93** (2016) 064304.
- [14] V.M. Kolomietz, A.I. Sanzhur, and S. Shlomo, Phys. Rev. C **97** (2018) 064302.
- [15] V. Zelevinsky and M. Horoi, Prog. Part. Nucl. Phys. **105** (2019) 180.
- [16] V.M. Kolomietz and S. Shlomo, *Mean Field Theory* (World Scientific, 2020).
- [17] V. Zelevinsky, B.A. Brown, N. Frazier, and M. Horoi, Phys. Rep. **276** (1996) 85.
- [18] J.M.G. Gomez, K. Kar, V.K.B. Kota, R. Molina, A.A. Relano, and J. Retamosa, Phys. Rep. **499** (2011) 103.
- [19] A.G. Magner, A.I. Levon, and S.V. Radionov, Eur. Phys. J. A **54** (2018) 214.
- [20] A.I. Levon, D. Bucurescu, C. Costache, T. Faestermann, R. Hertzenberger, A. Ionescu, R. Lica, A.G. Magner, C. Mihai, R. Mihai, C.R. Nita, S. Pascu, K.P. Shevchenko, A.A. Shevchuk, A. Turturica, and H.-F. Wirth, Phys. Rev. C **102** (2020) 014308.
- [21] V. Zelevinsky, S. Karampagia, and A. Berlaga, Phys. Lett. B **783** (2018) 428.
- [22] V.M. Kolomietz, A.G. Magner, and V.M. Strutinsky Sov. J. Nucl. Phys. **29** (1979) 758.
- [23] M. Brack, L. Damgaard, A.S. Jensen, A.C. Pauli, V.M. Strutinsky, and C.Y. Wong, Rev. Mod. Phys. **44** (1972) 320.
- [24] R. Balian and C. Bloch, Ann. Phys. **69** (1972) 76.
- [25] V.M. Strutinsky and A.G. Magner, Sov. J. Part. Nucl. **7** (1976) 138.
- [26] V.M. Strutinsky, A.G. Magner, S.R. Ofengenden, and T. Døssing, Z. Phys. A **283** (1977) 269.
- [27] M. Brack and R.K. Bhaduri, *Semiclassical Physics. Frontiers in Physics*, No. 96, 2nd ed. (Westview Press, Boulder, CO, 2003).
- [28] A.G. Magner, A.S. Yatsyshyn, K. Arita, and M. Brack, Phys. At. Nucl. **74** (2011) 1445.
- [29] W. Dilg, W. Shantl, M. Uhl, Nucl. Phys. A **217** (1973) 269.
- [30] B.K. Agrawal, S. Shlomo, and V.K. Au, Phys. Rev. C **72** (2005) 0114310.
- [31] M. Brack, C. Guet, and H.-B. Hakanson, Phys. Rep. **123** (1985) 275.
- [32] National Nuclear Data Center On-Line Data Service for the ENSDF database, <http://www.nndc.bnl.gov/ensdf>.